18TH WORLD CONFERENCE ON EARTHQUAKE ENGINEERING
WCEE2024
MILAN

MILAN, ITALY
30TH JUNE - 5TH JULY 2024
www.wcee2024.it

RELATIVE SUFFICIENCY OF DIFFERENT INTENSITY MEASURES FOR NATURAL AND SPECTRAL MATCHED GROUND MOTIONS RECORDS

C. Cantagallo[1], R. De Risi[2], M. Terrenzi[1], G. Camata[1] & E. Spacone[1]

[1] University "G d'Annunzio" of Chieti-Pescara, Department of Engineering and Geology, Pescara, Italy, e-mail: {cristina.cantagallo, marco.terrenzi, espacone, guido.camata}@unich.it

[2] University of Bristol, Department of Civil Engineering, Bristol, United Kingdom, e-mail: raffaele.derisi@bristol.ac.uk

Abstract: *A correct Intensity Measure (IM) selection is essential for Performance-Based Earthquake Engineering (PBEE) applications as the probabilistic seismic demand model (PSDM) depends significantly on the IM. If a single IM can describe the complexity of the corresponding ground motion record, it can be defined as sufficient in an absolute sense. However, this is unlikely because a single number should be able to inform on the frequency content, the amplitude, the duration, the energy content, etc. For this reason, literature studies have defined sufficiency in a relative sense to investigate whether one IM is more sufficient (i.e., more informative) than another in predicting the structural response. This work explores the relative sufficiency of eight scalar IMs through Nonlinear Response History Analyses (NRHAs) using two sets of 20 pairs of ground motion records. Both sets are spectrum-compatible, consisting of unscaled natural and spectral-matched records. Also, both Cloud and Incremental Dynamic Analysis procedures are used. It is demonstrated that the Cloud analysis cannot be used in its conventional form for the study of sufficiency when spectral-matched accelerograms are used. When natural accelerograms are employed, the results clearly indicate the existence of a sufficient IM among the selected. Conversely, for spectral-matched records, it is more difficult to define the relative sufficiency of the IMs because of the operation of record adjusting leading to similar structural demand. This result could question either the validity of using spectral-matched accelerograms for PBEE due to the lack of aleatory variability in the structural demand or the necessity of having a sufficient IM when a PSDM is fitted in a PBEE analysis using spectral-matched accelerograms.*

1 Introduction

In the framework of performance-based earthquake engineering (PBEE), seismic vulnerability is addressed by developing probabilistic seismic demand analyses (PSDA) and fragility curves that depict the conditional probability of the structure exceeding a certain limit state given the Intensity Measure (IM) of the ground motion (Porter, 2003). Thus, one of the essential criteria for reliable fragility and PSDA is the selection of appropriate IMs (Giovenale et al., 2004; Padgett et al. 2008). An inappropriate IM parameter may even make the entire hypothesis of the probabilistic seismic assessment invalid as IM relates in fact the seismic input and the seismic vulnerability analysis (Cantagallo et al., 2012; Huang et al., 2021). Therefore, selecting the best IM is a critical task that aids in increasing confidence in probabilistic seismic demand methods and subsequent risk assessments utilized in decision-making.

The criteria proposed in literature for measuring the suitability of an IM are expressed in terms of the information that it provides to predict the response quantities. Luco and Cornell (2007) and Jalayer et al. (2012) have proposed sufficiency as one of the most accurate criteria for measuring the suitability of an IM for representing the dominant features of ground shaking. More specifically, Jalayer et al. (2012) indicate that an IM is sufficient in an absolute sense if the damage measure conditional on this IM is dependent only on this IM and completely independent from other ground motion characteristics. As a result, establishing sufficiency in an absolute sense is nearly impossible unless using high-dimensional vector IMs. In general, for a scalar IM, the analysis of the relative sufficiency can be more interesting than the absolute one as it investigates whether one IM is more sufficient and more informative than another. The appropriateness of one IM relative to another for characterizing ground motion uncertainty was originally measured with the concept of entropy (Shannon, 1948; Jalayer and Beck, 2006), which measures the missing information that is required (on average) to specify the value of the uncertain variable. Based on the application of relative entropy, Jalayer et al. (2012) introduced a quantitative measure of the relative sufficiency to define how much information one IM gives relative to another about the considered damage measure. Subsequently, other research (Ebrahimian et al., 2015; Ebrahimian and Jalayer, 2020) apply the relative sufficiency measure to measure the suitability of alternative IMs in predicting various demand parameters. In these works, the IMs and the demand parameters are obtained using large sets of natural ground motion records that does not satisfy the spectrum-compatibility code requirements as they are selected on the basis of the only geophysical characteristics of the expected event (magnitude and epicentral distance). Current regulatory codes (ASCE/SEI 7-16 or Eurocode 8) typically specify a maximum misfit of individual response spectra or the average spectrum from a suite of motions compared to the code design spectrum. This requirement is aimed to reduce the dispersion in the elastic response spectra of the selected ground motion records and, consequently, the variability in the seismic demand, allowing the use of a limited number of records and analyses while having the same reliability (Hancock et al., 2008).

Since the spectrum-compatibility criterion required by the seismic codes is very difficult to satisfy, ground motion records are modified according to different criteria in engineering practice. One of the most common methods for modifying ground motion records is to linearly scale them to the target Peak Ground Acceleration PGA (i.e. to the PGA of the code design spectrum) (Nau and Hall, 1984) or to the spectral acceleration corresponding to the first period of vibration of the structure (Shome et al., 1988). However, even in this case, fulfilling the regulatory requirements is not easy unless high scale factors are used, significantly modifying the energy content of the motion records (Baker and Cornell, 2005; Cantagallo et al., 2015). As an alternative to scaling by a constant factor, the spectral matching method (Hancock et al., 2006; Bazzurro and Luco, 2006) is gaining attention among researchers and practitioners. This method is attractive because it minimizes the computational cost of selecting ground motion records according to the regulatory codes. The spectral-matching approach uses wavelets able to adjust the accelerograms so that their spectra match the target design spectrum minimizing changes to the other ground-motion characteristics (Romanelli et al., 2023). Currently, there are no works about the suitability of the spectral-matched records in evaluating the IM for PSDAs and fragility analysis.

This work aims to measure the suitability of different IMs obtained from both natural and spectral-matched records in predicting the structural response using the concept of relative sufficiency. The spectral-matched records are widely used in PSDAs and the derivation of fragility curves. For this reason, the analysis of the relative sufficiency of the IMs obtained with this ground motion selection and modification is becoming of increasing interest to the scientific community, as well as comparing the results obtained with natural records.

2 Description of the case study building

The case study building considered in this study is an existing reinforced concrete (RC) building designed in the 70s for only gravity loads according to old Italian codes (DM 30/05/1974). The plan layout of the building is rectangular with dimensions of 28.5x15.5 m. The total height is equal to 16m, corresponding to constant inter-storey heights of 3.2 m (Figure 1). The floor slabs are made of cast-in-place RC joists with hollow clay bricks between them and a thin, lightly reinforced concrete layer of 4 cm. The geometric configuration and the mass and stiffness distributions are symmetric with respect to the *x* and *y* reference axes shown in Figure 1. The structure is designed according to the allowable stress design principles (DM 30/05/1974). The section of the beams is 30x60 cm on all floors, while the column size decreases along the height of the building. For

more details about the case study building, and specifically about column sizes and element reinforcements, see (Cantagallo et al., 2023; Barbagallo et al., 2023).

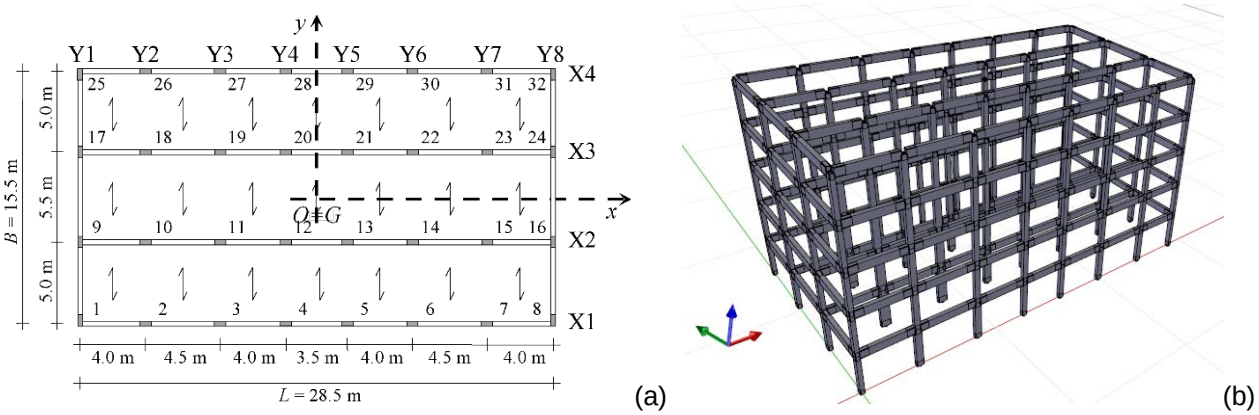

Figure 1. Plan layout (a) and 3D model (b) of the case study building.

3 Structural Model

The structural model and the non-linear analysis are carried out using the software platform OpenSees (McKenna et al., 2010) with the pre- and post-processor STKO (Petracca et al., 2017). The non-linear elements are modelled using *Beam-with-Hinges* elements (Scott and Fenves, 2006), in which a predefined plastic hinge length is assigned at the two ends, and the remaining element behaves as linear elastic. The end parts of the elements have a fibre-based discretization (Spacone et al., 1996) and a length equal to the cross-section height that, for rectangular sections, corresponds to the average dimension of the rectangle sizes. The inertia of the central elastic part of the element is reduced to account for cracking (50% E_cI_g for beams and 80% E_cI_g for columns, where E_c is the concrete elastic modulus and I_g is the gross section inertia) according to the suggestion of the current regulatory codes (NTC2018; ACI 318-19). The constitutive laws Concrete01 (Kent and Park, 1971) and Steel01 (Mazzoni et al., 2006) are used for modelling concrete and steel fibres, respectively. For the model Concrete 01 (OpenSees), the following input data are used: mean compressive strength f_{pc} = 28 *MPa*, strain at maximum strength ε_{c0} = 2.5‰, strain at crushing strength ε_{cu} = 3.5‰ and crushing strength f_{pcu} = 5.6 *MPa*. These data are used both in the core and cover section because the buildings designed according to the 70s regulatory codes (DM 30/05/1974) have stirrups with 90° rather than 135° hooks characterized by too large spacing for an effective confinement. Constitutive low Steel 01 is characterized by the following input data: elastic modulus E_s = 206000 *MPa*, yield strength f_y = 400 *MPa* and strain-hardening ratio b = 0.0049. The floor slabs are modelled by rigid diaphragms. These constraints prevent relative (in-plan) displacements between nodes of the same floor, generating fictitious axial forces in the beam elements. To overcome this problem, an axial release at the end of each floor beam is introduced. The fictitious axial force is eliminated by including an additional zero-length element with very low axial stiffness between one end of the beam and the adjacent node constrained to the rigid diaphragm (Barbagallo et al., 2020).

The first three linear periods of the structure are T_1 = 2.12 s, T_2 = 1.23 s and T_3 = 1.01 s, and the mass participation ratios in the structural directions U_x, Y_y, and R_z are $m_{1,Ux}$ = 0, $m_{1,Uy}$ = 78.7%, $m_{1,Rz}$ = 0, $m_{2,Ux}$ = 0, $m_{2,Uy}$ = 0, $m_{2,Rz}$ = 80.6%, $m_{3,Ux}$ = 79.0%, $m_{3,Uy}$ = 0, $m_{3,Rz}$ = 0, respectively, indicating that the first and the third mode are mainly translational and the second one is torsional. Gravity loads are applied statically on the structural model before the ground motion records are dynamically applied to the base of the structure.

4 Selection and modification of ground motion records

4.1 Natural ground motion records

Natural ground motion records are selected according to the Eurocode 8 (2005) and NTC2018 (2018) provisions. A reference site located at L'Aquila, AQ-Italy, 42.350° latitude and 13.399° longitude, on rock soil and an earthquake scenario corresponding to a probability of exceedance of 10% in 50 years are considered. In this contest, all the records with moment magnitude M_w between 5.5 and 7.6 and epicentral distance R between 3.4 and 53 km are pre-selected. Twenty ground motion records are then selected according to the

spectrum compatibility criterion so that, in the range of periods $0.2T_1$–$2T_1$, (where T_1 is the first period of vibration of the structure), the average spectrum calculated from all time histories is lower than the 90% of the corresponding target design spectrum. No upper bound is prescribed in Eurocode 8 (2005), while in the current study, a 110% upper bound to the existing 90% lower bound is added.). The spectrum-compatibility is obtained calculating for each ground motion a single response spectrum as the geometric mean $S_a(T)$ of the two horizontal spectral components $S_{aX}(T)$ and $S_{aY}(T)$ (Beyer and Bommer, 2006). The ground motion records are selected from the European Strong-motion Database ESD (Ambraseys et al., 2002) and the Engineering Strong-Motion database ESM (Luzi et al., 2016). The spectrum-compatibility check was carried out using spreadsheets created ad-hoc by the research group. Figures 2a) and 2b) show the comparison between the average spectrum obtained from the twenty selected ground motion records and the normalized target spectrum with a normal and lognormal plot, respectively. Each plot reports the geometric mean of the response spectra of each record (in grey), the target spectrum (in solid black), the average spectrum (in blue), the upper and lower limits (in dashed black) and the spectrum compatibility range (in dotted black).

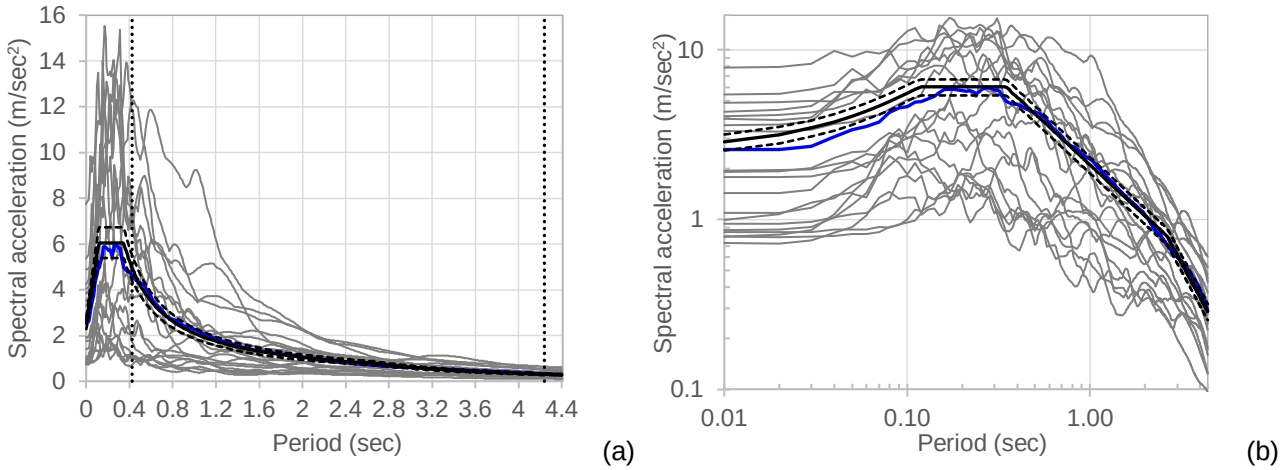

Figure 2. Selection of 20 real records: check of the spectrum-compatibility criterion by normal (a) and lognormal (b) plots.

4.2 Spectral-matched ground motion records

The twenty pairs of natural ground motion records selected according to the characteristics described in Section 4.1 are subsequently matched to the target spectrum with wavelet transforms. The wavelet transform consists of using modulating functions, selectively located in time to modify the spectrum of the signal, where and when it is needed, to match the target spectrum (Hancock et al. 2006). The matching of the time histories is carried out with the software SeismoMatch (Seismosoft, 2022) using the wavelets algorithm proposed by Al Atik and Abrahamson (2010) and a spectrum matching range [0.42–4.24] s. Figure 3a and Figure 3b check the spectrum-compatibility criterion with a normal and lognormal plot, respectively.

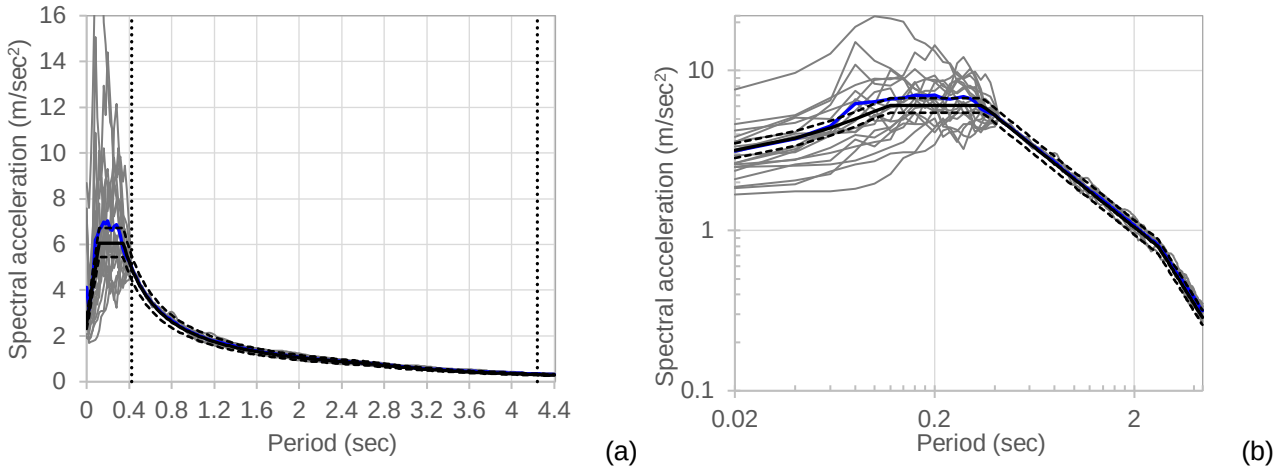

Figure 3. Selection of 20 spectral-matched records: check of the spectrum-compatibility criterion by normal (a) and lognormal (b) plots.

5 Intensity measures

In this study, eight different IMs are considered. Following the work of Mollaioli et al. (2013), these IMs are categorized into two groups: 1) non-structure-specific IMs, calculated directly from ground motion time histories and 2) structure-specific IMs, obtained from response spectra of ground motion time histories. Non-structure-specific IMs are further divided into acceleration-related IMs and velocity-related IMs. Structure-specific IMs are sorted into those obtained from the response spectral ordinate at certain periods and those obtained from the integration of response spectra. The variation of the IMs produced by the spectra-matching process on the IMs, and specifically on the energy intensity measures, is a measure of "distortion" of the original seismograms.

For each selected ground motion record, a single IM is obtained as the geometric mean of the two IMs calculated from the two horizontal ground motion components (Beyer and Bommer, 2006). The IMs values are determined using the software SeismoSignal (Seismosoft, 2018). In this study, the effect of the vertical component is not considered.

5.1 Non-structure-specific intensity measures

Acceleration-related Intensity Measures

The most commonly used measure of the amplitude of a particular ground motion is the Peak Ground Acceleration (PGA). The PGA for a given component of motion is the largest (absolute) value of acceleration obtained from the accelerogram $a(t)$ of that component.

$$\mathrm{PGA} = \max\left|a(t)\right| \tag{1}$$

The Arias Intensity (AI) is obtained as the integral of the square of the absolute acceleration time history (Arias, 1970). AI is an energy-based parameter that considers the amplitude and duration of the ground motion, but it is unable to capture the frequency characteristics of ground motions (Ghimire et al., 2021) and is not sensitive to long acceleration pulses in the excitation (Sucuoğlu and Nurtuğ, 1995).

$$\mathrm{AI} = \frac{\pi}{2g}\int_0^{t_{\max}} \left|a(t)\right|^2 dt \tag{2}$$

The Cumulative Absolute Velocity (CAV) is the area under the absolute accelerogram (EPRI, 1988):

$$\mathrm{CAV} = \int_0^{t_{\max}} \left|a(t)\right| dt \tag{3}$$

Velocity-related Intensity Measures

Specific Energy Density (SED) is the integral of the square of the absolute velocity time history $v(t)$. It is a measure of the overall energy of the record (larger SED, larger energy and expected damage).

$$\text{SED} = \int_0^{t_{max}} |v(t)|^2 \, dt \tag{4}$$

5.2 Structure-specific intensity measures

Spectral Intensity Measures

Two different spectral intensity measures are used in this work: the spectral acceleration corresponding to the first vibration period of the structure $S_a(T_1)$ (Nau and Hall, 1984) and the spectral acceleration corresponding to the structural period T^*, $S_a(T^*)$ (Cantagallo et al., 2012). T^* accounts for the elongation of the fundamental period during the non-linear analyses as it represents the period corresponding to the initial branch of the bilinear idealized capacity curve obtained from the non-linear static (pushover) analysis, according to Eurocode 8 (2005). As reported in Cantagallo et al. (2012), $S_a(T^*)$ is well correlated with the deformation demand and produces the lowest variability in structural demand among several intensity measures. The T^* values vary depending on the distribution of lateral loads and the loading direction. In this case, the T^* values are computed by applying a triangular load pattern to the considered case-study structure.

The case study structure is characterized by two different first periods of vibration T_1 in *x* and *y* directions, called T_{1x} and T_{1y}, respectively. After having calculated the response spectra corresponding to the two horizontal components of each selected record, the spectral accelerations $S_a(T_{1x})$ and $S_a(T_{1y})$ are obtained from the EW and NS horizontal components, respectively. $S_a(T_1)$ is then obtained as the geometric mean of $S_a(T_{1x})$ and $S_a(T_{1y})$ (Beyer and Bommer, 2006) to associate a single value of spectral acceleration to each record. The same procedure is adopted to obtain $S_a(T^*)$; in this case, T^*_x and T^*_y are obtained from non-linear static analyses carried out by applying triangular load patterns in the *x* and *y* structural directions.

Integral Intensity Measures

Von Thun et al. (1988) introduced the Acceleration Spectrum Intensity ASI, defined as the area under the acceleration response spectrum between periods of 0.1 s and 0.5 s.

$$\text{ASI} = \int_{0.1}^{0.5} S_a\left(\xi = 0.05, T\right) dT \tag{5}$$

Since many structures have fundamental periods between 0.1 and 2.5 s, the ordinates of the pseudo velocity spectrum in this period range should provide an indication of the potential response of these structures. For this reason, Housner (1959) defines the Hausner Intensity HI as the area under the 5% damped pseudo-velocity spectrum S_v in the period range [0.1-2.5s].

$$\text{HI} = \int_{0.1}^{2.5} S_v\left(\xi = 0.05, T\right) dT \tag{6}$$

6 Non-linear response history analyses

NRHAs are carried out by applying the selected combinations of ground motion records to the non-linear structural model. The analyses are carried out using a Rayleigh damping model with 2% damping (at the first and third mode frequency).

The results of NRHAs are reported and discussed here using the Maximum Interstorey Drift Ratio (MIDR = maximum interstorey reference point displacement/storey height) as the Engineering Demand Parameter (EDP). For each record, the interstorey drifts $\text{IDR}_X(t)$ and $\text{IDR}_Y(t)$ are computed from the centres of mass of two adjacent floors in the two structural direction X and Y, respectively. The IDR at an instant *t* is then computed as the SRSS combination of the interstorey drifts $\text{IDR}_X(t)$ and $\text{IDR}_X(t)$.

$$\text{IDR}(t) = \sqrt{\text{IDR}_X(t)^2 + \text{IDR}_Y(t)^2} \tag{7}$$

MIDR is calculated as the maximum IDR over time (the record duration); that is MIDR = max|IDR(*t*)|.

A single MIDR is obtained for each story and ground motion record. To consider a single EDP for each ground motion time history, the maximum MIDR of the five storeys of the case study building is finally calculated.

For a designated structural response parameter, such as θ_{max}, and the ground motion set of acceleration time histories ($\underline{\ddot{x}}_g$), the relative sufficiency IM_1 relative to IM_2 is obtained according to the formulation indicated in Jalayer et al. [10] and shown below:

$$I\left(\theta_{max} \mid IM_2 \mid IM_1\right) = E\left[D\left(\theta_{max} \mid IM_1 \mid \underline{\ddot{x}}_g\right) - D\left(\theta_{max} \mid IM_2 \mid \underline{\ddot{x}}_g\right)\right]$$
$$= \int \log_2 \frac{p\left(\theta_{max} \mid IM_2 \mid \underline{\ddot{x}}_g\right)}{p\left(\theta_{max} \mid IM_1 \mid \underline{\ddot{x}}_g\right)} \cdot p\left(\underline{\ddot{x}}_g\right) \cdot d\left(\underline{\ddot{x}}_g\right) \quad (8)$$

where $D\left(\theta_{max} \mid IM_i \mid \underline{\ddot{x}}_g\right)$ is the relative entropy.

The relative sufficiency $I(\theta_{max}|IM_2|IM_1)$ can be interpreted as a measure of how much information, on average, is gained about the uncertain structural response parameter θ_{max} by knowing IM_2 instead of IM_1.

If the relative sufficiency measure is zero, this indicates that on average the two IMs provide the same amount of information about θ_{max}. In other words, they are equally sufficient.

If the relative sufficiency measure is positive, this means that on average IM_2 provides more information than IM_1 about θ_{max}, so IM_2 is more sufficient than IM_1. Similarly, if the relative sufficiency measure is negative, IM_2 provides on average less information than IM_1 and so IM_2 is less sufficient than IM_1.

Table 1 and Table 2 show the values of relative sufficiency calculated from each pair of IMs obtained from the natural and the spectral-matched records, respectively. The positive values (pointed out in green) indicate that the IM reported in the first column is more sufficient (and therefore gives more information) than the IM of the first row. For example, the value of 0.2061 (fourth row, second column) indicates that SED provides more information than PGA about the MIDR. Conversely, negative values (in red) indicate that the IM is less sufficient than the other (the value of -0.2976 indicates that ASI provides less information than SED about the MIDR. The quantities shown in Table 1 and Table 2, on the other hand, reveal the measure of relative sufficiency by quantitatively indicating how much one IM provides more (or less) information than the other. For example, the values of the relative sufficiency of HI relative to AI and SED are 0.669 and 0.361, indicating that AI should contain more information than SED to represent the EDP uncertainty (i.e. the sufficiency of HI relative to AI is greater than the sufficiency of HI relative to SED).

Table 1. Relative sufficiency measures for IMs obtained from natural ground motion records.

IMs	PGA	AI	SED	CAV	HI	ASI	$S_a(T_1)$	$S_a(T^*)$
PGA	0.0000	0.1021	-0.2061	0.3396	-0.5672	0.0916	-0.7375	-0.3602
AI	-0.1021	0.0000	-0.3082	0.2375	-0.6694	-0.0105	-0.8396	-0.4624
SED	0.2061	0.3082	0.0000	0.5457	-0.3612	0.2976	-0.5315	-0.1542
CAV	-0.3396	-0.2375	-0.5457	0.0000	-0.9068	-0.2480	-1.0771	-0.6998
HI	0.5672	0.6694	0.3612	0.9068	0.0000	0.6588	-0.1703	0.2070
ASI	-0.0916	0.0105	-0.2976	0.2480	-0.6588	0.0000	-0.8291	-0.4518
$S_a(T_1)$	0.7375	0.8396	0.5315	1.0771	0.1703	0.8291	0.0000	0.3773
$S_a(T^*)$	0.3602	0.4624	0.1542	0.6998	-0.2070	0.4518	-0.3773	0.0000

Table 2. Relative sufficiency measures for IMs obtained from spectral-matched ground motion records.

IMs	PGA	AI	SED	CAV	HI	ASI	$S_a(T_1)$	$S_a(T^*)$
PGA	0.0000	0.0020	-0.0266	-0.0069	-0.0118	-0.0217	0.0046	-0.0396
AI	-0.0020	0.0000	-0.0286	-0.0090	-0.0139	-0.0238	0.0026	-0.0416
SED	0.0266	0.0286	0.0000	0.0197	0.0148	0.0049	0.0312	-0.0130
CAV	0.0069	0.0090	-0.0197	0.0000	-0.0049	-0.0148	0.0115	-0.0327
HI	0.0118	0.0139	-0.0148	0.0049	0.0000	-0.0099	0.0165	-0.0278
ASI	0.0217	0.0238	-0.0049	0.0148	0.0099	0.0000	0.0264	-0.0179

$S_a(T_1)$	-0.0046	-0.0026	-0.0312	-0.0115	-0.0165	-0.0264	0.0000	-0.0442
$S_a(T^*)$	0.0396	0.0416	0.0130	0.0327	0.0278	0.0179	0.0442	0.0000

Table 1 indicates that $S_a(T_1)$, $S_a(T^*)$ and HI are the most suitable intensity measures for natural and unscaled ground-motion records. The relative sufficiency values shown in Table 2 are all close to zero, leading to the impossibility of evaluating the most suitable IM to use in PSDM for spectral-matched records. The spectral-matching process significantly reduces the variability of both IMs and EDPs. The spectra of these types of time histories are made similar to each other with wavelet transforms. Consequently, the IMs and the corresponding MIDRs have minimum differences, and the relative sufficiency value becomes close to zero.

7 Incremental Dynamic Analyses

The relative sufficiency of the spectral-matched records is calculated using an IDA (Vamvatsikos and Cornell, 2002). In conventional IDA, a set of ground motions compatible with a design scenario is scaled to multiple intensity levels, and the structure response is evaluated at each intensity level. In this study, the set of twenty spectral-matched records is scaled so that the geometric mean of the spectral components has $S_a(T^*)$ varying from 0.1 to 4.0s., with a time step of 0.1 s. The scaling process of the spectral-matched records is an approximation due to the need to calculate the relative sufficiency of the spectral-matched records. In this work, IDA is used only as ground motions scaling approach to restore the ground motion variability of spectral matched records, and it is not finalized to the definition of fragility curves.

For each of the 400 scaled records, the eight considered IMs are obtained, and an NTHA is carried out to calculate the selected EDP. IDAs are also applied using the set of natural unscaled accelerograms to complete the work and validate the procedure. For low IMs (and scale factors), the MIDRs are well correlated with each considered IM. Conversely, when high-scale factors are applied, very high and irrealistic MIDRs are obtained, meaning the non-convergence of the solution.

To overcome the non-convergence issue, only the NTHAs carried out with accelerograms with scale factors lower or equal to 2.0 are considered for the calculation of the relative sufficiency. Note that in the range of scale factors [1.8, 2.0], only four records have non-convergence problems occurring after the time histories peak.

Table 3 and Table 4 show the relative sufficiency value obtained from the IDAs using natural and spectral-matched ground motion records, respectively. Red cells correspond to negative relative sufficiency values, green cells to positive values and black cells to null values. The results obtained for natural ground motion records indicate that, coherently with the results obtained by applying a single set of unscaled accelerograms, the IM with the highest relative sufficiency values is $S_a(T_1)$. The other two suitable IMs are ASI and $S_a(T^*)$. In this case, HI does not have high relative sufficiency values and cannot be considered a predictive IM. HI (Housner, 1952) is, in fact, defined as the area under the spectrum in pseudo-velocity in the range of periods [0.1, 2.5] s. The first period of vibration T_1 of the analyzed structure is equal to 2.12 s; for ground motion records characterized by high intensities and scale factors as those used in the IDAs, there is a significative elongation of T_1 and consequently, the range of periods considered by Housner (1952) loses its validity.

The relative sufficiency values obtained from the IDA applied using spectral-matched records confirm, in general, that the most suitable IMs are in $S_a(T_1)$, ASI and $S_a(T^*)$. Still, in this case, the IM with the highest relative sufficiency values is $S_a(T^*)$.

Table 3. Relative sufficiency measures for IMs obtained from natural ground motion records using IDAs.

IMs	PGA	AI	SED	CAV	HI	ASI	$S_a(T_1)$	$S_a(T^*)$
PGA	0.0000	0.0806	-0.0971	0.1940	0.1332	-0.1617	-0.2942	-0.0863
AI	-0.0806	0.0000	-0.1777	0.1134	0.0525	-0.2423	-0.3748	-0.1669
SED	0.0971	0.1777	0.0000	0.2911	0.2303	-0.0646	-0.1971	0.0108
CAV	-0.1940	-0.1134	-0.2911	0.0000	-0.0609	-0.3558	-0.4882	-0.2803
HI	-0.1332	-0.0525	-0.2303	0.0609	0.0000	-0.2949	-0.4273	-0.2194

ASI	0.1617	0.2423	0.0646	0.3558	0.2949	0.0000	-0.1324	0.0755
$S_a(T_1)$	0.2942	0.3748	0.1971	0.4882	0.4273	0.1324	0.0000	0.2079
$S_a(T^*)$	0.0863	0.1669	-0.0108	0.2803	0.2194	-0.0755	-0.2079	0.0000

Table 4. Relative sufficiency measures for IMs obtained from spectral-matched ground motion records using IDAs.

IMs	PGA	AI	SED	CAV	HI	ASI	$S_a(T_1)$	$S_a(T^*)$
PGA	0.0000	-0.0827	-0.1713	0.1411	-0.1873	-0.3801	-0.3731	-0.4034
AI	0.0827	0.0000	-0.0887	0.2238	-0.1046	-0.2974	-0.2905	-0.3207
SED	0.1713	0.0887	0.0000	0.3124	-0.0160	-0.2087	-0.2018	-0.2320
CAV	-0.1411	-0.2238	-0.3124	0.0000	-0.3284	-0.5211	-0.5142	-0.5444
HI	0.1873	0.1046	0.0160	0.3284	0.0000	-0.1927	-0.1858	-0.2160
ASI	0.3801	0.2974	0.2087	0.5211	0.1927	0.0000	0.0069	-0.0233
$S_a(T_1)$	0.3731	0.2905	0.2018	0.5142	0.1858	-0.0069	0.0000	-0.0302
$S_a(T^*)$	0.4034	0.3207	0.2320	0.5444	0.2160	0.0233	0.0302	0.0000

8 Conclusions

This paper applies the concept of relative sufficiency to calculate the most suitable IM for PSDAs when natural and spectral-matched ground motion records are employed. To this purpose, an existing building designed in the 70s for only gravity loads is selected as a case-study. The structure is analyzed with NTHAs using natural and spectral-matched ground motion records. Both sets of records consist of 20 pairs of horizontal accelerograms. After obtaining the MIDRs and eight different IMs for each considered time history, the corresponding values of relative sufficiency are calculated. For spectral-matched ground motion records, the relative sufficiency values are almost zero due to the wavelet transforms that generate a lack of variability in seismic input and consequently demand. IDAs are applied to the case-study structure to restore this variability using scaled spectral-matching records and calculating the corresponding relative sufficiency values. Finally, IDAs are also used to validate the method to calculate the relative sufficiency values for the IM obtained with natural and scaled ground motion records.

The main outcomes of the study are summarized hereafter:

- For unscaled natural ground motion records, the most suitable IMs to use for a PSDA or in general for predicting the seismic demand are $S_a(T_1)$, $S_a(T^*)$ and HI.
- When spectral-matched ground motion records are used, the IM values are very similar as well as the EDP values. The wavelet transform matches each spectrum to the target one, significantly reducing the variability of IMs and EDPs. In this case, the relative sufficiency values are almost null, and the estimation of the most suitable IM for spectral-matched time histories is not possible.
- The calculation of the relative sufficiency values of the IMs obtained from spectral-matched records is carried out using IDAs. In this case, the scaling process guarantees the variability of the ground motion records and the possibility of applying the relative sufficiency concept. For spectral-matched records the most sufficient and informative IMs to use in PSDA are $S_a(T_1)$, $S_a(T^*)$ and ASI.
- Applying the IDAs for calculating the relative sufficiency of the IMs obtained from natural ground motion records confirms $S_a(T_1)$ as the most sufficient and informative IM, validating the results obtained for the set of unscaled records. Other suitable IMs for a PSDA are $S_a(T^*)$ and ASI.

Future research should be developed to evaluate as the lack of variability in spectral-matched records could further influence a PSDA and the PBEE applications.

9 References

Al-Atik L., Abrahamson N.A.(2010). An improved method for nonstationary spectral matching. *Earthq. Spectra*, 26(6): 601–617.

Ambraseys N., Smit P., Sigbjornsson R., Suhadolc P., Margaris B. (2002). Internet-Site for European Strong-Motion Data, European Commission, Research-Directorate General, Environment and Climate Programme.

Arias A. (1970). *A measure of earthquake intensity*. In: Hansen RJ (ed) Seismic design for nuclear power plants. MIT, Cambridge, MA, pp 438–483.

ACI 318-19 (2019). *Building Code Requirements for Structural Concrete and Commentary*; American Concrete Institute: Farmington Hills, MI, USA.

ASCE/SEI 7-16 (2017). *Minimum design loads and associated criteria for buildings and other structures*. American Society of Civil Engineers (ASCE), Reston, VA. https://doi.org/10.1061/9780784414248.

Baker J.W., Cornell, A.C. (2005). A vector‐valued ground motion intensity measure consisting of spectral acceleration and epsilon. *Earthquake Engineering & Structural Dynamics*, 34(10): 1193-1217.

Barbagallo F., Bosco M., Marino E.M., Rossi P.P. (2020). On the fibre modelling of beams in RC framed buildings with rigid diaphragm. *Bulletin of Earthquake Engineering*, 18(1):189-210. doi: 10.1007/s10518-019-00723-z

Barbagallo F., Di Domenico M., Terrenzi, M., Cantagallo C., Marino E.M., Ricci P., Verderame G.M., Camata G. and Spacone E. (2023). Influence of the modelling approach on the seismic assessment of RC structures by nonlinear static analyses. *Soil Dynamics and Earthquake Engineering*, 172: 107970. https://doi.org/10.1016/j.soildyn.2023.107970.

Bazzurro P, Luco N. (2006). Do scaled and spectrum-matched near-source records produce biased nonlinear structural responses? *Proceedings of the 8th National Conference on Earthquake Engineering*, 18-22.

Beyer K., Bommer J.J. (2006). Relationships between median values and between aleatory variabilities for different definitions of the horizontal component of motion, *Bulletin of the Seismological Society of America*, 96(4A): 1512–1522.

Cantagallo C., Camata G., Spacone E., Corotis, R. (2012). The variability of deformation demand with ground motion intensity, P*robabilistic Engineering Mechanics*, 28: 59–65. https://doi.org/10.1016/j.probengmech.2011.08.016.

Cantagallo C., Camata G., Spacone, E. (2015). Influence of ground motion selection methods on seismic directionality effects. *Earthquakes and Structures*, 8(1): 185. https://doi.org/10.12989/eas.2015.8.1.185.

Cantagallo C., Terrenzi M., Barbagallo F., Di Domenico M., Ricci P., Camata G., Spacone E., Marino E.M. and Verderame G.M. (2023). Effects of the extended N2 method on non-linear static procedures of reinforced concrete frame structures. *Soil Dynamics and Earthquake Engineering*, 173: 108144. https://doi.org/10.1016/j.soildyn.2023.108144.

Ebrahimian H., Jalayer F., Lucchini A., Mollaioli F., Manfredi G. (2015). Preliminary ranking of alternative scalar and vector intensity measures of ground shaking. *Bulletin of Earthquake Engineering*, 13, 2805-2840.

Ebrahimian H., Jalayer F. (2021). Selection of seismic intensity measures for prescribed limit states using alternative nonlinear dynamic analysis methods. *Earthquake Engineering & Structural Dynamics*, 50(5), 1235-1250.

Electrical Power Research Institute (EPRI) (1988). A criterion for determining exceedence of the operating basis earthquake. EPRI NP-5930, EPRI, Palo Alto, CA.

European Committee on Standardization (CEN), 2004. UNI EN 1998-1:2005, *Eurocode 8: Design of structures for earthquake resistance - Part 1: General rules, seismic actions and rules for buildings*, EN1998-1, Brussels.

Ghimire S., Guéguen P., Astorga A. (2021). Analysis of the efficiency of intensity measures from real earthquake data recorded in buildings. *Soil Dynamics and Earthquake Engineering*, 147: 106751.

Giovenale P., Cornell C.A., Esteva L. (2004). Comparing the adequacy of alternative ground motion intensity measures for the estimation of structural responses. *Earthquake engineering & structural dynamics*, 33(8): 951-979.

Hancock J., Watson-Lamprey J., Abrahamson N.A., Bommer J.J., Markatis A., McCoy E.M.M.A., Mendis R. (2006). An improved method of matching response spectra of recorded earthquake ground motion using wavelets. *J. Earthquake Eng.*, 10(1): 67–89.

Hancock J., Bommer J.J., Stafford P.J. (2008). Numbers of scaled and matched accelerograms required for inelastic dynamic analyses. *Earthquake Engineering and Structural Dynamics*, 37(14):1585–1607.

Housner G.W. (1952). Spectrum intensities of strong-motion earthquakes. In *Proceedings Symposium on Earthquake and Blast Effects on Structures*; Earthquake Engineering Research Institute: Los Angeles, CA, USA.

Huang Z.K., Pitilakis K., Argyroudis S., Tsinidis G., Zhang D.M. (2021). Selection of optimal intensity measures for fragility assessment of circular tunnels in soft soil deposits. *Soil Dynamics and Earthquake Engineering*, 145: 106724.

Jalayer, F., Beck, J.L. (2006). Using information theory concepts to compare alternative intensity measures for representing ground motion uncertainty. In *Proc., 8th US National Conf. Earthquake Engineering*, Paper ID (Vol. 974).

Jalayer F., Beck J.L., Zareian F. (2012). Analyzing the sufficiency of alternative scalar and vector intensity measures of ground shaking based on information theory. *Journal of Engineering Mechanics*, 138(3): 307-316.

Kent D.C., Park R. (1971). Flexural members with confined concrete. *Journal of the Structural Division*, ASCE; 97:ST7. doi: 10.1061/JSDEAG.0002957.

Luco N., Cornell, C.A. (2007). Structure-specific scalar intensity measures for near-source and ordinary earthquake ground motions. *Earthquake Spectra*, 23(2): 357-392.

Luzi L., Puglia R., Russo E. (2016). *ORFEUS WG5. Engineering Strong Motion Database*, version 1.0. Istituto Nazionale di Geofisica e Vulcanologia, Observatories & Research Facilities for European Seismology. doi: 10.13127/ESM.

Mazzoni S., McKenna F., Scott M.H., Fenves G.L. (2006). *OpenSees command language manual*. Pacific Earthquake Engineering Research (PEER) Center, 264:137-158.

McKenna F, Scott M.H., Fenves G.L. (2010). Nonlinear finite-element analysis software architecture using object composition. *Journal of Computing in Civil Engineering*, 24(1): 95-107. doi: 10.1061/(ASCE)CP.1943-5487.0000002.

Ministero dei lavori pubblici, Decreto ministeriale del 30/05/1974, *Norme tecniche per la esecuzione delle opere in cemento armato normale e precompresso e per le strutture metalliche*, Gazzetta Ufficiale Serie generale n. 198 del 29/07/1974, Roma (in Italian).

Mollaioli F., Lucchini A., Cheng Y., Monti G. (2013). Intensity measures for the seismic response prediction of base-isolated buildings. *Bulletin of Earthquake Engineering*, 11: 1841-1866.

Nau, J. M., Hall, W. J. (1984). Scaling methods for earthquake response spectra. *J. Struct. Eng.*, 110(7): 1533–1548.

NTC2018 (D.M. 17/01/2018). Decreto del Ministero delle Infrastrutture e dei trasporti del 17/01/2018. *Aggiornamento delle Norme Tecniche per le Costruzioni*, Gazzetta Ufficiale Serie generale n. 42 del 20/02/2018, Roma (in Italian).

Padgett J.E., Nielson B.G., DesRoches R. (2008). Selection of optimal intensity measures in probabilistic seismic demand models of highway bridge portfolios. *Earthquake engineering & structural dynamics*, 37(5): 711-725.

Petracca M., Candeloro F., Camata G. (2017). *STKO user manual*. ASDEA Software Technology, Pescara.

Porter K. (2003) An overview of PEER's performance-based earthquake engineering methodology. *Proc. ninth Int. Conf. Appl. Stat. Probab. Civ. Eng*. (ICASP9), San Fr. 2003.

Romanelli F., Vaccari F., Cantagallo C., Camata G., Panza G.F. (2023). Physics-Based Approach to Define Energy-Based Seismic Input: Application to Selected Sites in Central Italy. In: Varum, H., Benavent-Climent, A., Mollaioli, F. (eds) Energy-Based Seismic Engineering. IWEBSE 2023. *Lecture Notes in Civil Engineering*, vol 236. Springer, Cham. https://doi.org/10.1007/978-3-031-36562-1_9.

Scott M.H., Fenves G.L. (2006). Plastic Hinge Integration Methods for Force-Based Beam-Column Elements. *Journal of Structural Engineering*, 132(2): 244-252. doi: 10.1061/(ASCE)0733-9445(2006)132:2(244).

Seismosoft (2022) – *SeismoMatch - A Computer Program for Spectrum Matching of Earthquake Records* (2022). Available from URL: https://seismosoft.com/

Seismosoft (2018). *SeismoSignal - A computer program for signal processing of time-histories*. Available from URL: https://seismosoft.com/

Shannon C.E. (1948). A mathematical theory of communication. *Bell system technical journal*, 27(3), 379-423.

Shome N., Cornell C.A., Bazzurro P., Carballo J.E. (1998). Earthquakes, records, and nonlinear responses. *Earthq. Spectra*, 14: 469–500.

Spacone E., Filippou F.C., Taucer .FF. (1996). Fibre beam‐column model for non‐linear analysis of R/C frames: Part I. Formulation. *Earthquake Engineering & Structural Dynamics*, 25(7): 711-725. doi: 10.1002/(SICI)1096-9845(199607)25:7<711::AID-EQE576>3.0.CO;2-9.

Sucuoğlu, H., Nurtuğ, A. (1995). Earthquake ground motion characteristics and seismic energy dissipation. *Earthquake engineering & structural dynamics*, 24(9): 1195-1213.

Vamvatsikos D., Cornell C.A. (2002). Incremental dynamic analysis. *Earthquake engineering & structural dynamics*, 31(3): 491-514.

Von Thun J.L., Roehm L.H., Scott G.A., Wilson J.A. (1988). Earthquake ground motions for design and analysis of dams. In: *Proceedings of the earthquake engineering and soil dynamics II-recent advances in ground motion evaluation*, Geotechnical Special Publication, ASCE, New York, pp 463–481